

Small-scale variability of orographic precipitation in the Alps: Case studies and idealized simulations for the National Park Berchtesgaden area

Günther Zängl



Introduction

One of the major difficulties in studying small-scale precipitation variability in mountainous terrain is that current rain gauge networks are usually not dense enough to fully resolve this variability. This is partly because surface stations tend to be clustered at easily accessible valley locations whereas slope and mountain locations are largely underrepresented. For convective precipitation, radar measurements can fill this gap to a large extent, but the situation is not as good for precipitation variability related to the seeder-feeder mechanism, because the related precipitation enhancement is usually concentrated to fairly low elevations above ground and thus is difficult to detect with operational radar measurements. The main goal of this study is to examine to what extent high-resolution numerical simulations are able to generate realistic small-scale precipitation patterns, which could afterwards be used for a spatial interpolation of point measurements such as needed for climatologies or hydrological modelling. The present work focuses on the National Park Berchtesgaden in southeastern Germany, the region with the densest operational rain gauge network in the whole Alps. Here, two heavy-precipitation cases (10–12 July 2005 and 15–17 August 2005) are examined that were characterized by a fairly unusual small-scale rainfall distribution. The real-case simulations are complemented by a number of semi-idealized simulations, combining realistic topography with idealized large-scale flow conditions.

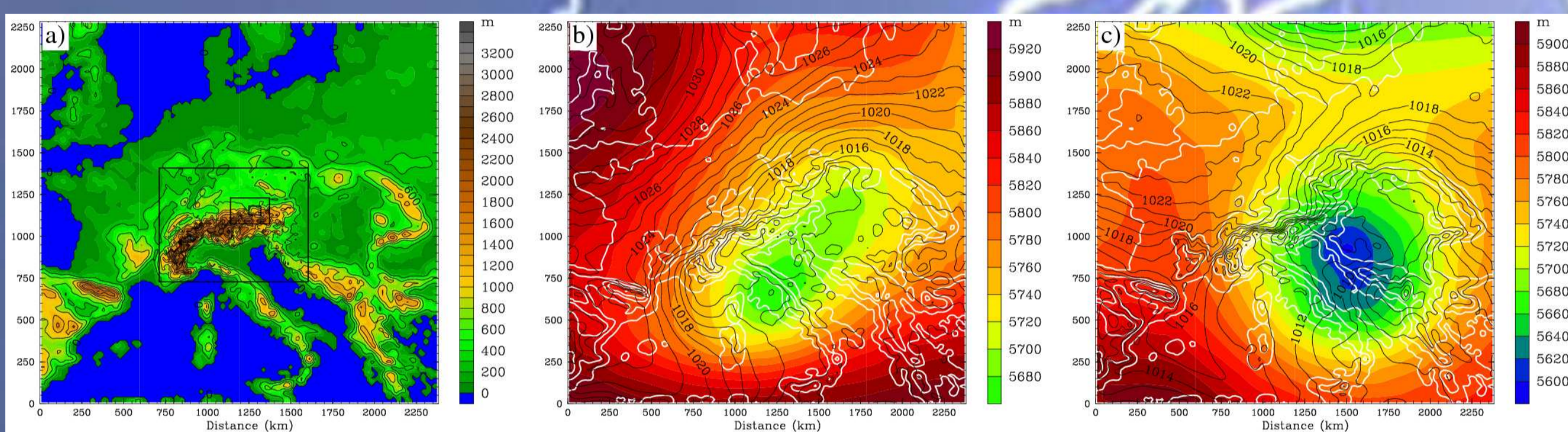


Fig. 1: (a) Topography of the coarse model domain and location of the nested domains (boxes); (b,c) 500-hPa geopotential height (colours) and sea-level pressure (contour interval 1 hPa) at 00 UTC 11 July 2005 and 06 UTC 16 August 2005, respectively.

Model and setup

The numerical simulations presented here have been conducted with the Penn State / NCAR mesoscale model MM5, version 3.6. Four two-way nested model domains are used with a finest mesh size of 600 m. The area covered by the coarsest domain (domain 1) is displayed in Fig. 1a including the positions of the nests. To allow for a realistic description of the relevant physical processes, a complete set of physics parameterizations for cloud micro-physics, subgrid-scale convection, radiation and boundary-layer processes is used. The initial and boundary conditions used for the real-case simulations are obtained from operational ECMWF data. The simulations start at 00 UTC 10 July 2005 and 12 UTC 15 August 2005, respectively, and are conducted for 54 h and 42 h, respectively. The synoptic situations during these cases are illustrated in Fig. 1b,c. For the semi-idealized simulations, synthetic large-scale fields are prescribed as shown in Fig. 2. Two different temperature profiles are considered, starting from a sea-level temperature of 285 K and 275 K, respectively. The lapse rate depends on pressure and is kept slightly below the moist adiabatic one, and the relative humidity is set to 98% in the lower and middle troposphere. The ensuing θ_e profiles are shown in Fig. 2a. The wind profiles are characterized by positive vertical shear and a clockwise turning with height (Fig. 2b,c). The clockwise turning, corresponding to warm-air advection via the thermal wind relation, is used as a simple way to enforce large-scale lifting. This turned out to be important for obtaining realistic precipitation patterns. The wind direction will be referred to by its value at 700 hPa (360° in Fig. 2c in the remainder of this paper. It will be varied between 315° and 30° and appears in the simulation name together with the acronyms given in Fig. 2 for the temperature and wind profiles (see caption of Fig. 4).

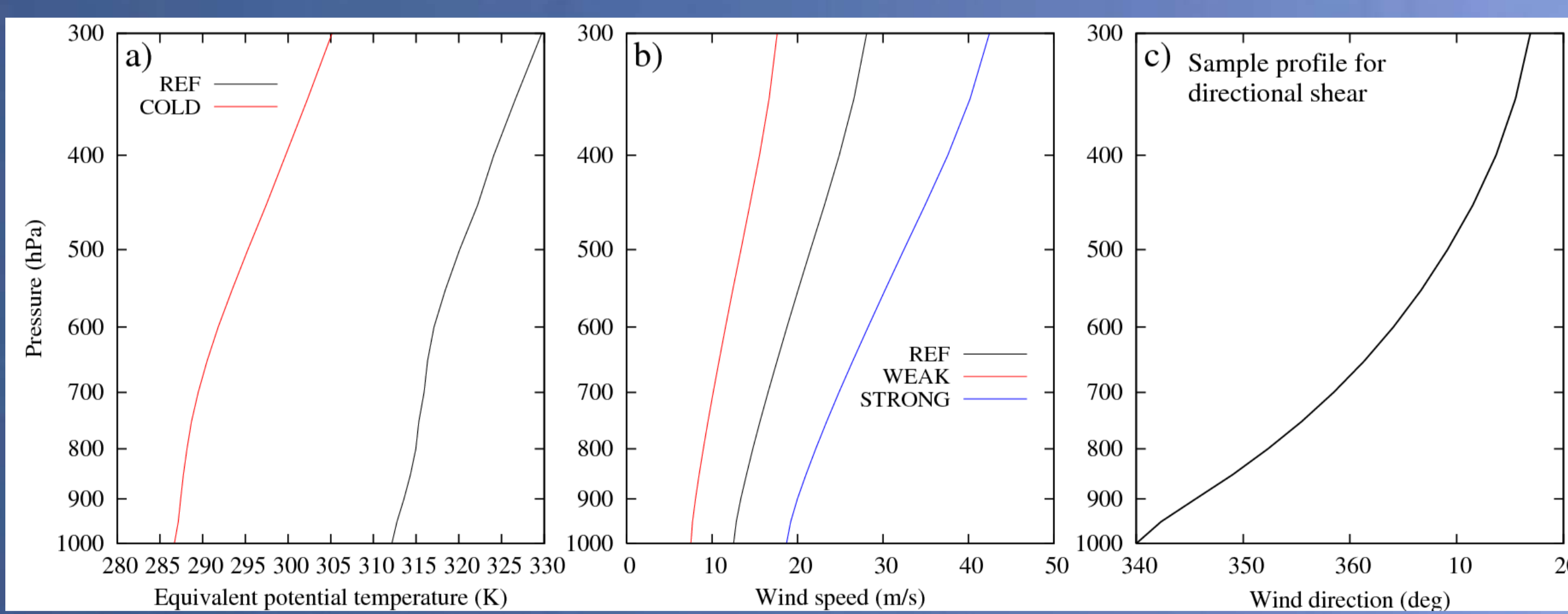


Fig. 2: Profiles of large-scale atmospheric parameters for semi-idealized simulations; (a) equivalent potential temperature, (b) wind speed, (c) wind direction for a 700-hPa direction of 360°. The acronyms used in the line keys also appear in the simulation names used in the discussion and Fig. 4.

Results

The most striking feature of the observed precipitation fields (Fig. 3a,b) is a pronounced precipitation maximum at a station located on the southwestern flank of a major mountain massif (the Untersberg massif near Salzburg), far exceeding the values recorded at all surrounding stations. Apart from that, there is a tendency for higher rainfall accumulations at the inner-Alpine stations than close to the northern edge of the Alps, particularly in case 1 (Fig. 3a). The sim-

ulations reproduce the primary precipitation maximum at the Untersberg massif, but its magnitude is underpredicted in case 1 (Fig. 3c) and overpredicted in case 2 (Fig. 3d). A closer analysis of the model results reveals that these maxima are generated by the classical seeder-feeder mechanism, combined with downstream advection of the precipitation hydrometeors. On average over the whole domain, the canonical correlation coefficient between simulated and observed precipitation amounts to 0.73 for case 1 and 0.71 for case 2.

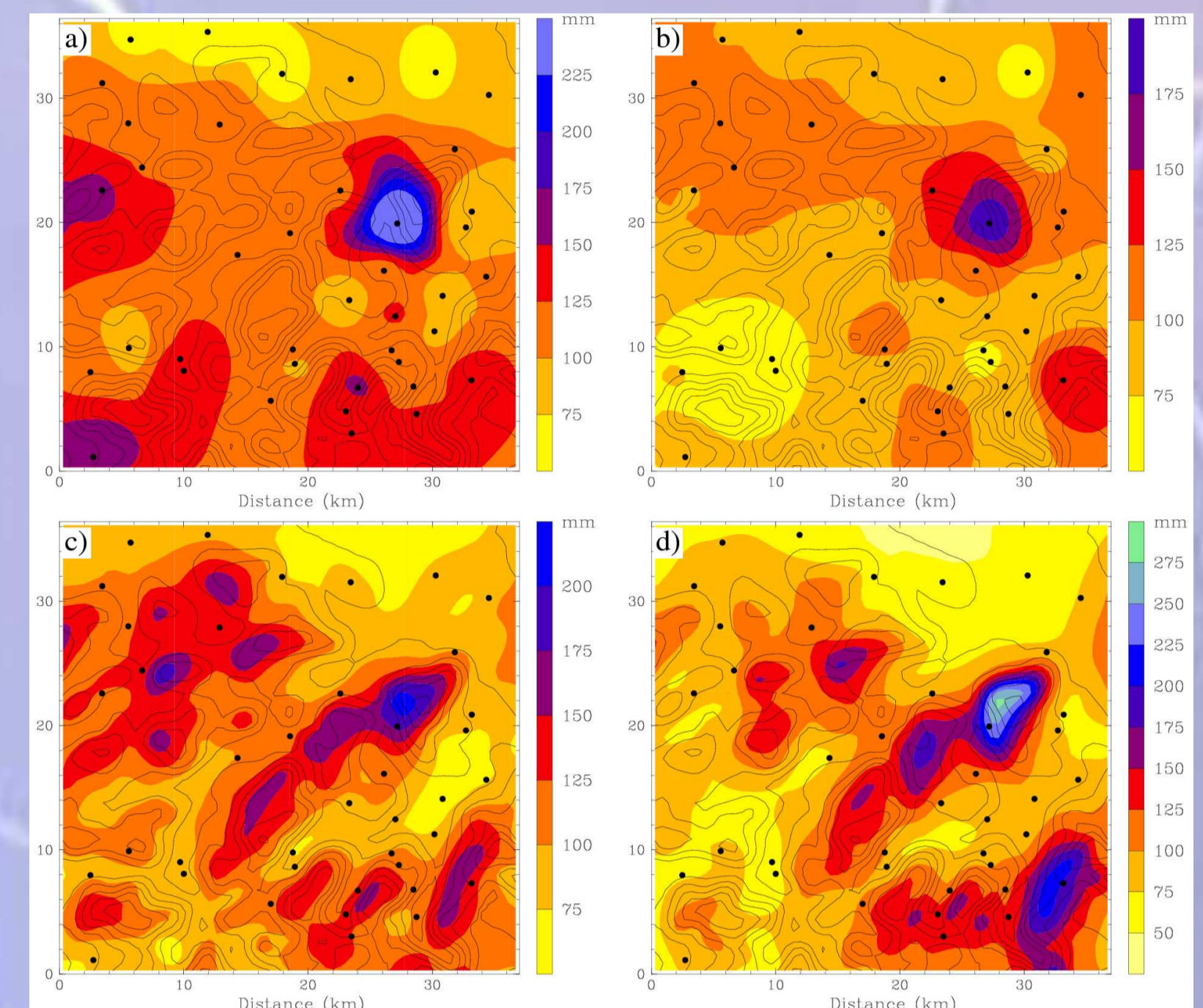


Fig. 3: Observed (upper panels) and simulated (lower panels) storm-total precipitation for case 1 (left) and case 2 (right).

To obtain further information on the factors controlling the small-scale variability patterns, semi-idealized simulations have been conducted. The REF temperature and wind profiles (Fig. 2a,b) have been specified such as to approximately match those observed in the real cases. The real 700-hPa wind direction was about 30° in case 1 and 15° in case 2. The precipitation fields obtained from the semi-idealized simulations are shown in Fig. 4, accumulated over 24 h of simulation and scaled to a domain-average value of 100 mm (which is close to what occurred in the real cases). The patterns obtained for 700-hPa wind directions of 15° and 30° (Fig. 4b,c) are indeed fairly similar to those from the real-case simulations for case 2 and case 1, respectively, whereas a completely different pattern is obtained for 315° (run 315-REF, Fig. 4a). This indicates that the ambient wind direction plays an important role in setting up the small-scale rainfall patterns. Changing the temperature or the wind speed has a smaller but still substantial impact. Specifically, decreasing the temperature by about 10 K ("COLD" in Fig. 2a) decreases the magnitude of the major precipitation peaks (Fig. 4d, cf. with Fig. 4b), and there are some moderate structural changes due to the lower freezing level. The general decrease of the precipitation amount (by a factor of about 2.4) does not appear in Fig. 4 due to the above-mentioned scaling. Decreasing the ambient wind speed (Fig. 4e, 015-WEAK) also reduces the local peaks and leads to relatively more precipitation near the northern edge of the Alps, whereas increasing the ambient wind (Fig. 4f, 015-STRONG) increases the peaks and shifts the precipitation into the interior of the Alps due to a stronger downstream advection of the hydrometeors. The correlation between the precipitation fields of 015-REF and 030-REF and the real-case data turned out to be similar as for the corresponding real-case simulations. Changing the ambient flow conditions strongly degrades the correlation, particularly for wind direction.

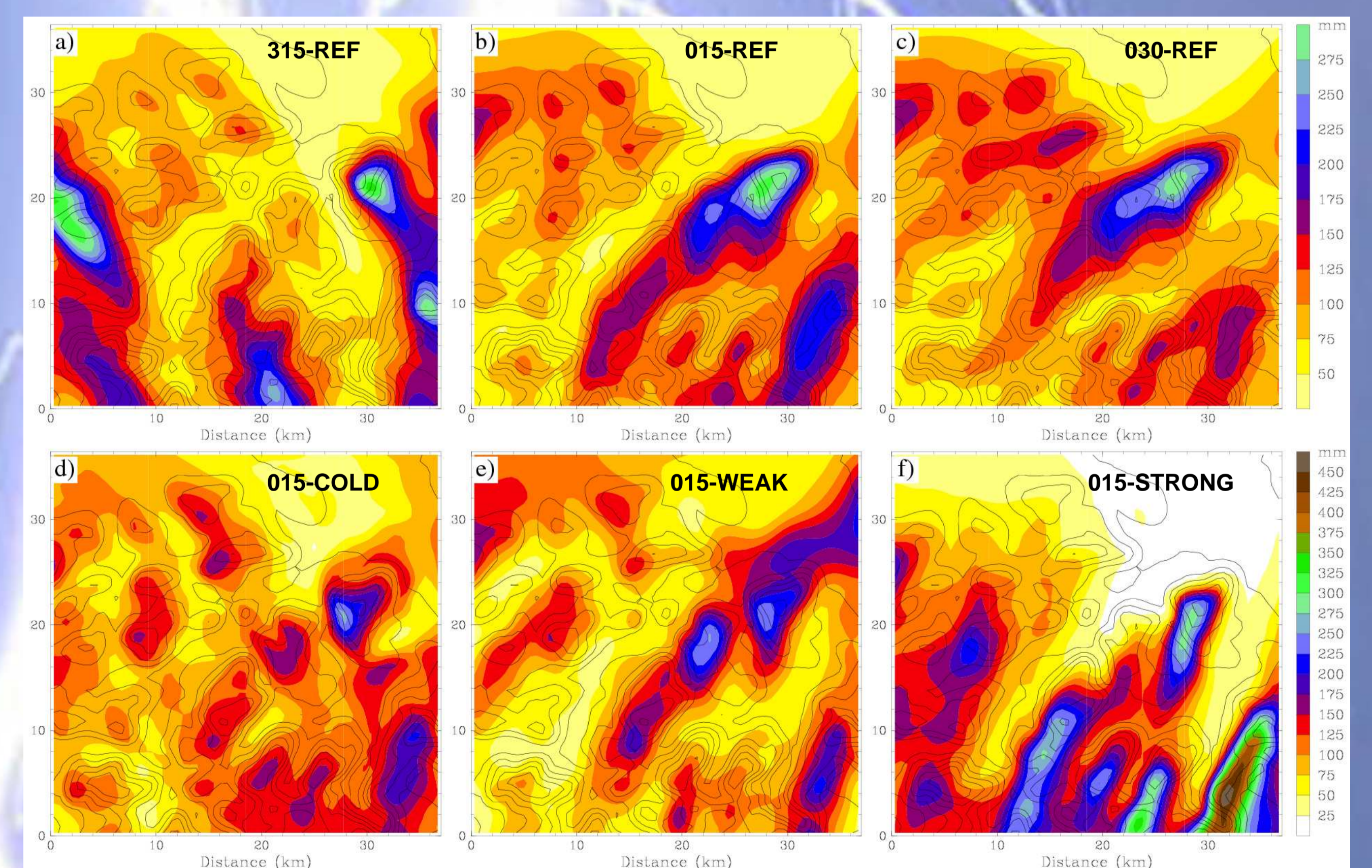


Fig. 4: Simulated 24-h accumulated precipitation for semi-idealized simulations, scaled to a domain average of 100 mm for cases (a) 315-REF, (b) 015-REF, (c) 030-REF, (d) 015-COLD, (e) 015-WEAK and (f) 015-STRONG. See Fig. 2 for the corresponding large-scale conditions.

For further information see:

Zängl, G., 2007: Small-scale variability of orographic precipitation in the northern Alps: Case studies and idealized numerical simulations. Submitted to *Quart. J. Roy. Meteor. Soc.*